International Journal of Pharmaceutics 615 (2022) 121506

Contents lists available at ScienceDirect

International Journal of Pharmaceutics

journal homepage: www.elsevier.com/locate/ijpharm

On the progress of hydrogel-based 3D printing: Correlating rheological properties with printing behaviour

Sara Bom [a,1], Ricardo Ribeiro [a,1], Helena M. Ribeiro [a], Catarina Santos [a,b,c,*], Joana Marto [a,*]

[a] Research Institute for Medicines (iMed.ULisboa), Universidade de Lisboa, 1649-003 Lisboa, Portugal
[b] CQE, Instituto Superior Técnico, Universidade de Lisboa, Av. Rovisco Pais 1049-001, Lisboa, Portugal
[c] EST Setúbal, CDP2T, Instituto Politécnico de Setúbal, Portugal

ARTICLE INFO

Keywords:
Printability
Extrudability
Printing accuracy
Shape fidelity
Printing precision

ABSTRACT

One of the exciting future directions in the 3D printing field is the development of innovative personalized smart constructions for bio-applications, including drug delivery, namely high-throughput drug screening and customized topical/oral administration of pharmaceuticals, as well as tissue engineering. In this context, hydrogels have emerged as a promising material that, when combined with extrusion 3D printing, allow the creation of soft-material structures with defined spatial locations, that can be printed at room temperature and customized by tuning the geometric design and/or the formulation components. Thus, the efficacy and quality of such vehicles is dependent on formulation, design, and printing process parameters. However, hydrogel inks are often designed and characterized using different methods and this lack of uniformity impairs. Characterization techniques are usually arbitrary and differ among research groups, challenging the inference of possible conclusions on hydrogel behaviour and potential applications. Therefore, to properly analyse the potential of a particular hydrogel ink formulation, we review, for the first time, the most frequently employed characterization procedures, from rheological approaches to printing parameters and settings, and discuss their relevance, limitations and drawbacks, and highlight future perspectives. Overall, to accelerate the development of high-quality 3D constructs, comprehensive characterization protocols for both pre-printing and printing assays should be adopted. Furthermore, their transversal adoption could serve as a boost in terms of quality requirements and regulatory aspects.

1. Introduction

3D Printing is an additive manufacturing process in which a 3D construct is generated layer-by-layer, based on a computer-aided design (CAD) model (Bom et al., 2021; Ngo et al., 2018; Ozbolat et al., 2016; Pati et al., 2015; Song et al., 2010; Wang et al., 2015; You et al., 2017). However, this technology is not limited to one technique, instead offering a panoply of methods, that can be divided in seven main categories: powder-based printing (binder jet printing), extrusion-based printing (fused deposition modelling (FDM) and hydrogel-forming extrusion (HFE)), stereolithographic printing (SLA), selective laser sintering printing (SLS), inkjet printing (IJ), and digital light processing (DLP) (Azad et al., 2020; Bom et al., 2020; Derakhshanfar et al., 2018; Kirchmajer et al., 2015; Ngo et al., 2018; Vithani et al., 2019; Wang et al., 2015). Among these, 3D printing-based HFE has been leading to growing interest in various fields such as oral and topical/transdermal drug delivery, tissue engineering, regenerative medicine, and biological-based therapies, due to the ability of printing semi-solid or solid 3D constructs (simple or complex vehicles or devices) at room temperature using a wide range of polymers (Bom et al., 2021, 2020; Economidou et al., 2018; Gu et al., 2020; Kirchmajer et al., 2015; Kotta et al., 2019; Ngo et al., 2018; Prasad and Smyth, 2016; Wang et al., 2015).

Abbreviations: CAD, Computer-aided Design; FDM, Fused Deposition Modelling; HA, hyaluronic acid; HFE, Hydrogel-forming Extrusion; SLA, Stereolithography; SLS, Selective Laser Sintering; IJ, Inkjet Printing; DLP, Digital Light Processing; UV, Ultraviolet; POI, Parameter Optimization Index; TSS, Theoretical Shear Stress; LVER, Linear Viscoelastic Region; PCL, Polycaprolactone; PEG, Polyethylene Glycol; PEGDA, PEG diacrylate; PTRI, Printing Temperature Range Interval; CFD, Computational Fluid Dynamics; NO, Nozzle Offset; NG, Nozzle Geometry; CT, Computed Tomography; MRI, Magnetic Resonance Imaging.

* Corresponding authors.
E-mail addresses: sarabom@campus.ul.pt (S. Bom), ris.ribeiro@campus.fct.unl.pt (R. Ribeiro), hribeiro@campus.ul.pt (H.M. Ribeiro), catarina.santos@estsetubal.ips.pt (C. Santos), jmmarto@ff.ulisboa.pt (J. Marto).

[1] Both authors contributed equally to this work.

https://doi.org/10.1016/j.ijpharm.2022.121506
Received 16 October 2021; Received in revised form 17 January 2022; Accepted 20 January 2022
Available online 24 January 2022

Furthermore, HFE enables the printing of different layers composed by different materials within a single construct, being considered a very versatile manufacturing approach (Firth et al., 2018; Gillispie et al., 2020).

The process of introducing a new medicine to the market is laborious and frequently challenged by failure in late-stage trials (Peng et al., 2017). 3D bioprinting is an emerging alternative that combines drug discovery and drug delivery, through the creation of advanced and/or biomimetic constructs, creating an ideal platform for high-throughput drug screening via microarrays in different tissue development stages, with increased insight over traditional 2D models due to a closer resemblance to the native tissue architecture, although it still battles some trade-offs such as limited resolution and reproducibility (Ozbolat et al., 2016; Peng et al., 2017). Hence, printing is valuable for pre-clinical drug assessment, including efficacy and toxicity studies. Moreover, drug-loaded hydrogels are fine-tunable by varying parameters such as crosslinking degree, polymer concentration and molecular weight, allowing the optimization of drug delivery strategies, both from a general and a personalized point-of-view (Lee et al., 2019). Although, it is possible to realize that HFE 3D printing technologies have come to revolutionize the pharmaceutical and biomedical fields, with the potential to completely change design, manufacturing, and prescription paradigms (Trenfield et al., 2018). Nevertheless, hydrogel printing is not an easy task since this type of polymeric solutions are mostly composed of water molecules and/or other solvent-like compounds (Wang et al., 2015), which can hinder the achievement of adequate printing accuracy and shape fidelity (upon deposition). In addition, the hydrogels' viscoelastic properties can hamper the printing of tall structures (over 1 cm) or complex structures with well-defined angles or even circular, also depending on the printer's resolution (Gillispie et al., 2020). As a result, most polymeric hydrogel inks are not self-supporting and tend to collapse or spread substantially after printing due to gravitational forces (leading to an overall loss of structure by means of compression or sagging) and surface tension (Gillispie et al., 2020; Ribeiro et al., 2017). Therefore, hydrogels often cannot maintain its 3D shape (Skardal et al., 2016), and secondary interventions may be necessary to promote the gelation of the hydrogel inks resorting to physical, ionic, or radiation crosslinking (Cui et al., 2020; Gillispie et al., 2020; You et al., 2017). Considering ionic crosslinking, 3D extrusion printers that simultaneously print the hydrogel and the ionic solution (coaxial printing or dual printing) already exist. In addition, some printers have UV light incorporated in the extrusion head, allowing the crosslink to be performed at the end of the printing procedure, between each layer or directly in the extruding filament. Consequently, the *modus operandi* of the printer, and the type of settings it provides, can also be considered parameters that influence the printing quality.

Overall, the challenges inherent to the semi-solid extrusion 3D printing technology over other 3D printing methods, go from the hydrogel intrinsic properties to the need of a secondary crosslinking strategy, the knowledge over the printer settings, and the adoption of reliable and standardized characterization methods. Thus, and as discussed so far, ensuring printing quality is a fundamental prerequisite for the success of HFE 3D printed constructs. However, by analysing the most recent literature on this subject, it is clear that there is still misinformation and a lack of uniformity of concepts and analysis methodologies to be adopted (Lee et al., 2018; You et al., 2017). In addition, and as previously mentioned by Naghieh *et al.* (Naghieh et al., 2019) and Gillispie *et al.* (Gillispie et al., 2020), although there are several studies reporting the 3D printing extrusion of different polymeric materials, the real picture and the definition of printing quality remain unclear, leaving essential questions on how to categorize the relationships between printability and other interrelated factors, such as physicochemical, rheological, morphological, and mechanical properties of 3D printed constructs. For example, some authors use a rheological approach to describe printability, while others have been focusing on studying the influence of ionic crosslinkers, nozzle variables, material composition, pore and filament dimensions, geometry, and printing angle on printing quality, as well as in the gelation properties of materials during the printing process (Cai et al., 2020; Freeman and Kelly, 2017; He et al., 2016; Magalhães et al., 2019; You et al., 2017). However, considering only one of the factors is not a systematic approach to improving printing quality. In addition, when choosing different analysis and characterization strategies, authors preclude a reliable comparison of data. Understanding the influence of the most diverse variables interlinked with the overall 3D printing process can be critical to ensure the printing of high-quality 3D constructs and to ensure their functionality and application features.

This article presents and discusses the most relevant parameters that influence the printing quality ranging from pre-printing (rheological parameters and nozzle selection) to printing (pressure and nozzle offset optimization, shape fidelity and printing accuracy tests). An additional section discusses the limitations and drawbacks of the most common methods used for characterization and optimization of hydrogel inks printed through 3D HFE-based printing techniques and presents future perspectives.

2. 3D Hydrogel-forming extrusion (HFE)

2.1. Printing concept and hydrogel-forming polymers

The 3D HFE printing process describes the computer-controlled layer-by-layer dispensing of semi-solid (molten or semi-molten) polymeric solutions, dispersions or pastes through a movable nozzle in (x,y, z) coordinates, create a 3D structure. The associated term "hydrogel-forming" implies the use of polymers that react by means of physical, ionic, or radiation crosslinking, allowing the gelation of the 3D printed construct (Godoi et al., 2016). Hydrogel-forming polymers can be classified either considering their source (synthetic, natural or hybrid/modified), ionic charge (non-ionic, cationic, anionic or ampholytic), biodegradability (biodegradable or non-biodegradable), physical properties (smart or conventional), electrostatic nature and/or gel-forming mechanism (physical, chemical or radiation crosslinking) (Kirchmajer et al., 2015; Lee et al., 2018; Li et al., 2020). A wide variety of polymers are currently exploited for HFE 3D printing, including those of natural origin such as gelatin, alginate, fibrin, starch, and chitosan, and those of synthetic origin such as polyethylene glycol (PEG) or polycaprolactone (PCL). Chemical/physical modified (e.g., gelatin methacryloyl and pregelatinized starch) or hybrid polymers (e.g., PEG diacrylate (PEGDA) crosslinked with hyaluronic acid (HA)) with unique properties, have also gained a lot of attention since their use can improve the physicochemical properties of the hydrogel and/or the 3D construct functionality and applicability (Bom et al., 2020; Carrow et al., 2015). The advantages and disadvantages of the different polymers available for HFE have been extensively reviewed elsewhere (Cui et al., 2020; Gopinathan and Noh, 2018; Li et al., 2020) and will not be extensively discussed in this review article. Briefly, the criterion for selecting a polymer is dependent on features such as the biocompatibility, production method and cost, rheological and mechanical features, extrusion mechanism, the desired applicability and functionality of the 3D construct, the crosslinking mechanism of the polymer, and several others (e.g., sustainability concerns).

2.2. Printers

Common extrusion-based 3D printers can be classified according to the printing driven system into pneumatic, mechanical (piston and screw-driven) or solenoid-based systems (Fig. 1) (Bedir et al., 2020; Boularaoui et al., 2020; Firth et al., 2018; Gu et al., 2020; Lee et al., 2018; Li et al., 2020; Pati et al., 2015; Seoane-Viaño et al., 2021). To streamline, pneumatic extrusion 3D printers use compressed air to dispense the ink, *via* an on-off valve switching control or valve-free system, that is directly connected to the cartridge (Firth et al., 2018;

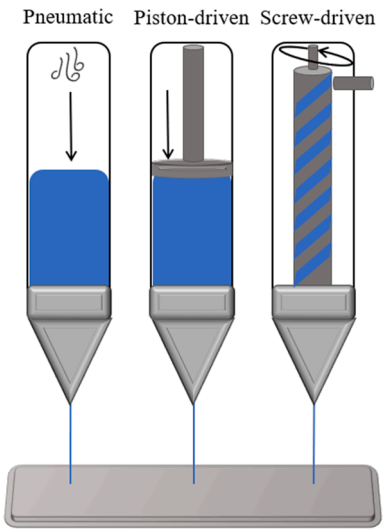

Fig. 1. Representation of the mechanism in three distinct extrusion-based printing techniques: pneumatic, piston-driven and screw-driven extrusion.

Gu et al., 2020). The valve switching control is highly recommended for low-viscosity inks to prevent dispensing when no pressure is being employed; for high-viscosity materials, valve-free systems can be considered, because the flow rate when no pressure is applied (only considering gravitational forces) is neglectable (Firth et al., 2018). The use of pneumatic-driven systems provides a high degree of precision associated with the extrusion control process, as well as a faster response time after the start of the extrusion process, since the cartridge can be pressurized instantly, and significant pressures can be achieved without compromising the integrity of the 3D constructs (Firth et al., 2018). Mechanical-driven extrusion systems apply a mechanical force directly to the cartridge, providing a much simpler mechanism than the one used in pneumatic extrusion. In piston-driven systems, a piston is coupled to a motor employing a guide screw and when the motor starts, the rotational movement of the guide screw is transferred to the linear movement of the piston, which pushes the ink out of the nozzle, starting ink extrusion. The concept of a screw-driven system is similar to a piston-driven one, except that the screw, which is connected to the motor, is used directly for extrusion, as a substitute of a piston (Gu et al., 2020). The piston-driven system provides enhanced control over the extrusion flow, whilst the screw-driven system delivers superior spatial control and is more efficient to dispense materials with higher viscosities than the piston-driven systems. The overall mechanism is simpler than the pneumatic one, and is more affordable and easier to transport, eliminating the necessity of utilizing an air compressor device (Firth et al., 2018). The solenoid systems work through electrical pulses that are directed to a valve located at the base of the syringe (Boularaoui et al., 2020; Firth et al., 2018; Seoane-Viaño et al., 2021). Besides the differences in the *modus operandi* and in advantages/disadvantages, pneumatic-driven systems are more suitable for printing hydrogels with shear-thinning properties, piston and screw-driven systems are more suitable for extrusion of high viscosity inks, and solenoid systems are more suitable for low viscosity inks that require ionic or UV crosslinking (Boularaoui et al., 2020; Firth et al., 2018; Gu et al., 2020; Seoane-Viaño et al., 2021).

3. Print quality

Ensuring print quality is one of the main challenges when considering an HFE-based 3D printing technique since hydrogels are mainly composed of water which can inherently hamper the printing of high-quality, accurate and reproducible 3D constructs. Furthermore, it is essential to understand in-depth the concept of print quality for future translation of 3D printed constructs to the market (approval and commercialization). The question then is, what is considered print quality? Does it depend exclusively on the hydrogel characteristics (rheological behaviour, mechanical properties, and crosslinking method), and/or also on printing parameters? How can it be defined? Print quality is a concept that is poorly defined in literature, without standardized nomenclature and procedures, with different authors describing different ways of evaluating such a concept. Although some authors have already discussed this topic and have proposed more accurate definitions in an attempt to standardize concepts, these are not yet consensual, due to the fast-growing increase in 3D printing research. Thus, to overview in-depth the concept of print quality, a survey of the most used terms in the literature was carried out, which will be further discussed.

The concept of print quality can cover definitions such as printability (most cited), printing accuracy, printing precision, printing fidelity, extrudability, extrusion uniformity, structural integrity and construct integrity. Within this tangle of definitions, **printability** is the one that causes more misunderstanding in the literature, because this word, which was initially used to describe the relative ability of paper to take printed ink, was adopted for 3D printing contexts independently of the resources, materials and techniques used. Thus, and as each type of 3D printing technique has a specific set of requirements (from materials to printing mechanism), the word acquired many different meanings that also change depending on the planned application, further complicating the understanding of the term (Gillispie et al., 2020; Naghieh and Chen, 2021). The word printability, according to its etymology, is the ability to print (Lee et al., 2020). In a 3D printing context, however, it refers to the ability of a material to be used in a layer-by-layer system to create a 3D object according to a computer-defined design. However, some authors go beyond this basic definition and try to detail it further, to increase the perception of the term. Agarwal *et al.* (Agarwal et al., 2021), defined printability as "an extent of the ease of printing bioink formulations, specific to each bioprinter type". According to Godoi *et al.* (Godoi et al., 2016), printability depends on the material and can be affected by its rheological properties, gelification mechanisms (crosslinking) and thermal properties. The definition of Theus *et al.* (Theus et al., 2020) was based on the previous one (Godoi et al., 2016) but considered surface tension a critical factor, in addition to the rheological properties. Li *et al.* (Li et al., 2020) also considered that the printability of hydrogel materials is dependent on the rheological properties (viscosity, shear-thinning behaviour, yield stress) and crosslinking mechanisms. Furthermore, and according to Murphy and Atala (Murphy and Atala, 2014), printability can be defined as "properties that facilitate handling and deposition by the bioprinter, which may include viscosity, gelation methods and rheological properties.", whilst highlighting the influence of print time and nozzle gauge on printability. Gopinathan and Noh (Gopinathan and Noh, 2018) described printability as being dependent on distinct parameters such as viscosity and the surface tension of the bioink, crosslinking ability, or surface properties of the printer nozzle, whereas for Gillispie *et al.* (Gillispie et al., 2020), printability is considered the ability to achieve desirable printing outcomes under a set of printing conditions, in a particular application. To minimize further misunderstanding the authors also clarified the meaning of printing conditions (which relate to process parameters, including printing settings and environmental conditions) and printing outcomes (referring to the measures of success for the printing procedure). Thus, instead of considering printability only as a parameter that depends exclusively on the characteristics of the material, several authors also include in their definition the influence of the printing parameters/settings (e.g., feed rate, pressure, construct design, nozzle geometry and printing temperature). For example, Suo *et al.*, describes printability as dependent on the extrusion state of the needle, where: a) a extrudate in the form of a droplet can be considered unprintable; b) a lumpy extrudate can cause nozzle clogging; and, c) a smooth, silky and filamentous extrudate is considered printable (Suo et al., 2021). Thus, for some researchers the

definition of printability is purely qualitative or determined by visual analysis (which can sometimes lead to ambiguity), with no general consensus. To solve this doubtfulness, some authors underlined the need of establishing and adopting a semi-quantitative or quantitative definition of printability to improve and facilitate the development, characterization and optimization of high-quality and reproducible 3D constructs. Ouyang *et al.* (Ouyang et al., 2016) developed a new semi-quantitative method for evaluating printability based on rheological measurements and image analysis (perimeter and area determination), which has already been used by several authors in recent papers (Cai et al., 2020; Habib et al., 2018; Habib and Khoda, 2018; Kreller et al., 2021; Soltan et al., 2019). For a quantitative definition of printability index (Pr), the authors proposed the following equation (for squared shapes) – Fig. 2 (A):

$$Pr = \frac{\pi}{4} \times \frac{1}{C} = \frac{L^2}{16A}, \quad (1)$$

where C is the circularity of an enclosed area ($C = \frac{4\pi A}{L^2}$), L stands for perimeter and A for area.

Naghieh *et al.* (Naghieh et al., 2019) suggest measuring printability based on the following equations:

$$Nozzlespeed = \frac{4Q}{\pi(Ds)^2}, \quad (2)$$

where, Q and Ds are flow rate and standard strand diameter, respectively.

Based on the nozzle speed equation, strand printability was defined as:

$$Strandprintability = 1 - \frac{Ds - Dexp}{Dexp}, \quad (3)$$

where Dexp refers to the experimental strand diameter.

Despite the usefulness and significance of the proposed mathematical equations, they do not fully reflect all factors that can interfere with printability, in addition to being based exclusively on measurement parameters in (x,y) (which are inaccurate to evaluate layer stacking in multilayer printing). Thus, and given the complex nature of the printability concept, several other concepts or indexes have emerged.

Printing accuracy, the second most cited definition in the literature, is normally used to describe how similar the printed construct is to the CAD drawing in terms of geometry and spatial resolution. Gillispie *et al.* (Gillispie et al., 2020) considered that printing accuracy is the degree to which printed constructs match their intended size, shape, and location when applying determined printing parameters. For Webb and Doyle (Webb and Doyle, 2017), printing accuracy is a direct result of the geometry of printed lines and is dependent on the pressure applied to the fluid. According to the fluid mechanics principle, an increase in printing pressure or a decrease in nozzle diameter increases shear stress, which is undesirable during the printing process. To maximise printing accuracy and minimise theoretical shear stress (TSS), the same authors developed a Parameter Optimization Index (POI). The POI can be determined through the following equations:

$$POI = Accuracy \times \frac{1}{TSS} \quad (4)$$

$$TSS = \frac{1}{DG \times p}, \quad (5)$$

where DG represents the nozzle gauge and p represents pressure.

$$Accuracy = \frac{1}{tline}, \quad (6)$$

where tline corresponds to line thickness.

Hence, the POI can be expressed as:

$$POI = \frac{1}{tline \times DG \times p} \quad (7)$$

In the study by Kang *et al.* (Kang et al., 2013), the authors evaluated print accuracy, print resolution and layer thickness by defining dimensionless variables indexes of length, width, and height, respectively. To assess print accuracy the authors used the length index L' (Fig. 2(B)):

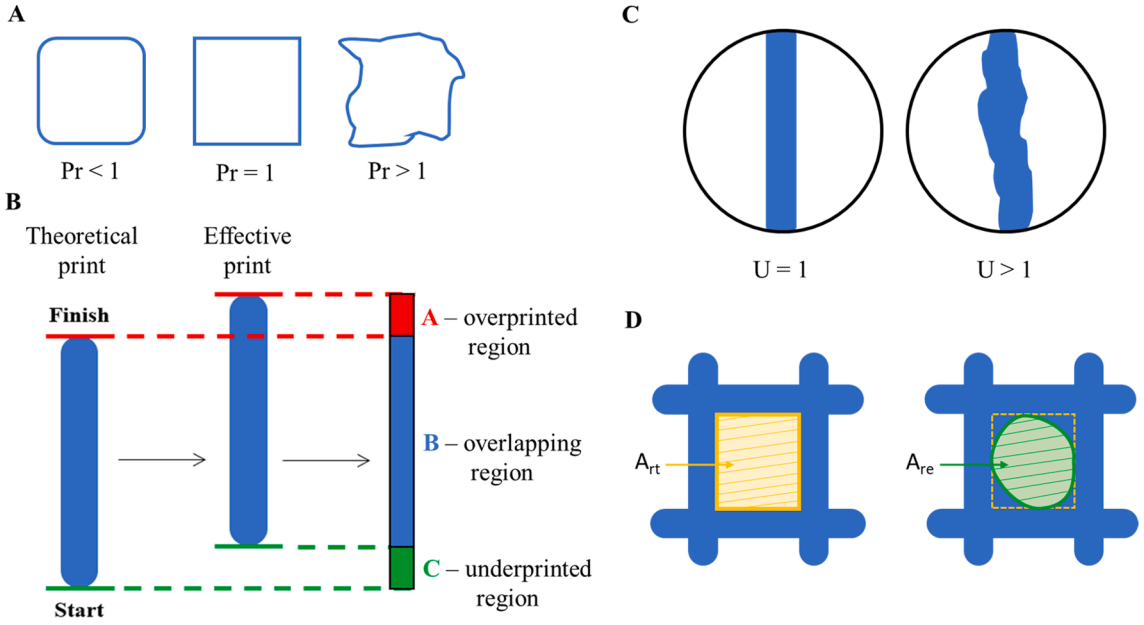

Fig. 2. Different printability formulas used in recent research. (A) Application of the printability formula for pores, developed by Ouyang *et al.* (Ouyang et al., 2016), in which a Pr = 1 corresponds to a properly gelled, Pr < 1 means under-gelled and Pr > 1 to an over-gelled ink. **(B)** Illustration of the L' index suggested by Kang *et al.* (Kang et al., 2013), that allows to categorize the offset in length between the designed and the printed path. **(C)** Illustration of a nonuniform (U > 1) and a uniform strand filament (U = 1). **(D)** Method proposed by He *et al.* (He et al., 2016) to assess shape/printing fidelity, in which ratios closer to 0 depict enhanced printing fidelity.

$$L' = \frac{C}{A + B + C'}, \tag{8}$$

where A = average underprinted, B = overlapping and C = overprinted length of the printed construct.

Print resolution was evaluated through the width index W':

$$W' = \frac{Wavg}{D}, \tag{9}$$

where D = nozzle diameter and Wavg = average construct width between n samples.

To investigate layer thickness the height index H' was used:

$$H' = \frac{T}{H}, \tag{10}$$

where H = construct height and T = average thickness.

Another term that is often referred to in the literature is **printing fidelity** or shape fidelity, which describes the ability of a hydrogel ink to maintain its shape following deposition. According to Gillispie *et al.* (Gillispie et al., 2020), printing fidelity can be analysed whilst using a single layer, such as by measuring the dimensions of printed filaments, and can be interpreted by measuring phenomena like spreading ratio, height maintenance, and/or filament collapse. Schwab *et al.* (Schwab et al., 2020) discussed the influence of rheological factors on printing fidelity and reviewed the most common assessment approaches used to evaluate printing this parameter in planar and multilayer structures. As for rheological factors, viscosity is considered the one that mostly influences shape fidelity, with higher viscosities resulting in higher printing fidelity. Furthermore, the authors stated that "shear-thinning behaviour and rapid, reversible sol-gel transition are key factors in defining printability and shape fidelity in extrusion printing". In terms of methods for evaluating shape fidelity, the authors highlighted the possibility to measure three distinct parameters depending on the structure to be printed: i) filament circularity, which is directly related to the geometric macroscopic shape, and describes the phenomenon of filament spreading on a surface; ii) pore geometry, which describes the degree of reproducing ideal pore geometric shapes, allowing to evaluate the spreading and fusion of filaments at the intersection – it is applicable to constructs of either single or multi-layered structure in order to identify the quality of layer stacking; and, iii) visual grid, which permits the direct comparison of printed structures to computer-generated lattices, although limited to uncomplicated constructs with macroscopic porosity.

To assess filament uniformity, Soltan *et al.* (Soltan et al., 2019) defined uniformity factor as (Fig. 2(C)):

$$U = \frac{lengthofprintedstrand}{lengthoftheoreticalstraightstrand} \tag{11}$$

For open-pore (or lattice) structures, Habib *et al.* (Habib and Khoda, 2018) defined the diffusion rate, also known as rate of material spreading, according to the equation below:

$$Dfr(\%) = \frac{At - Aa}{At} \times 100 \tag{12}$$

where At = theoretical area and Aa = actual area.

Kim *et al.* (Kim et al., 2019) used the following equation to evaluate printing fidelity:

$$Printingfidelity(\%) = \frac{Printedporearea}{Designedporearea} \times 100 \tag{13}$$

He *et al.* (He et al., 2016) also defined a mathematical expression to evaluate the 3D constructs lattice quality, which could be related with printing quality/ fidelity (Fig. 2(D)):

$$\varphi = \frac{Art - Are}{Art}, \tag{14}$$

where Art is the theoretical area of a lattice and Are is the experimental area of the lattice.

Sarker and Chen (Sarker and Chen, 2017) developed a mathematical model based on the relationship between the flow rate and printing speed. Based on this, Theus *et al.* (Theus et al., 2020) described that the printing fidelity of the printed filament (diameter, Dp) can be calculated by the equation (15) ignoring the swelling and gravity effects:

$$Dp = \sqrt{\frac{4Q}{\pi Vp}}, \tag{15}$$

where Q is the volumetric flow rate and Vp represents the printing speed.

Curti *et al.* (Curti et al., 2021) also evaluated the dimensional stability (Δd) by measuring the dimensional changes (length, L, width - W, height - H) before and after rehydration of the printed samples, using a simple equation:

$$\Delta d(\%) = \frac{dr - d0}{d0} \times 100 \tag{16}$$

where d0 is the initial L/W/H of dried samples and dr is the measured L/W/H after samples rehydration.

Extrudability is another concept derived from printability, which evaluates the capability to achieve adequate extrusion. According to Gao *et al.* (Gao et al., 2019), extrudability can be defined as the minimum pneumatic pressure required to extrude the ink at a constant flow rate. The authors further used the terms "extrusion uniformity" and "structural integrity". In this context, there is also another term called "construct integrity" that refers to the ink capability of holding its structure after printing through area (x,y) measurements.

To facilitate the comprehension of print quality, as well as to standardize and reduce the number of concepts used in the literature, we propose the adoption of only the following concepts: printability, extrudability, printing accuracy, printing/shape fidelity, and printing precision, which translate the essentials that must be considered in an HFE-based 3D printing process. The definitions of the proposed concepts are summarized in Table 1.

These concepts will be used, accordingly, throughout this review article to facilitate the interpretation of the following sections.

Table 1
Definition of concepts related to the printing quality.

Concept	Definition
Printability	The ability of a certain ink to achieve extrusion and maintain shape fidelity with high printing accuracy, which is influenced by pre-printing (rheological and nozzle features), printing [design, slicing, g-code (e.g., pressure, temperature and feed rate) and non-g-code parameters (e.g., environmental conditions)] and post-printing parameters (e.g., crosslinking, coating or drying techniques).
Extrudability	The capability of achieving extrusion, which is influenced by rheological parameters, printing parameters and environmental conditions.
Printing accuracy	Degree to which the 3D printed construct matches their size and spatial location, with respect to the original CAD model in terms of length, width, and height.
Printing fidelity	Degree to which the 3D printed construct matches their geometry with respect to the original design file in terms of length and width.
Printing precision	Measures the repeatability or reproducibility of a print in terms of size, geometry, and spatial location.

4. 3D printing process optimization

4.1. 1. Pre-printing

4.1.1. Rheology

Overall, rheology studies the deformation and the flow of hydrogels in response to forces applied. In an HFE-based process, the ink is initially in a bulk resting state (no flow) inside the cartridge, and when forces are applied, it transitions to endure deformation and flow in high shear conditions while moving through the nozzle walls. Subsequently, it acquires a new shape until it finally returns to a new resting state (Fig. 3) (Schwab et al., 2020; Seoane-Viaño et al., 2021). The pivotal rheological properties which relate to these transitions are viscosity, the viscoelastic shear moduli, the viscosity recovery behaviour, and shear stress, which can be associated with the ink's performance before (rest and flow initiation), during (flow behaviour - extrudability) and after printing (printing accuracy, shape fidelity and adhesiveness) (Amorim et al., 2021; Schwab et al., 2020). The key rheological parameters that describe these phenomena are discussed below, as well as the most used tests for their characterization, including rotational and oscillatory methodologies.

4.1.1.1. Flow behaviour. Newtonian fluids possess a linear relationship between the rheological elements of shear stress and shear rate, whereas fluids depicting deviations to that linearity are described as non-Newtonian. These can be further classified into time-independent (e.g., shear-thinning and shear-thickening) or time-dependent fluids (e.g., thixotropic or antithixotropic) (Fig. 4(A)) (Cooke and Rosenzweig, 2021; Schwab et al., 2020; Shahbazi and Jäger, 2021).

The behaviour of Newtonian fluids can be described through the Newton's law (Chhabra and Richardson, 1999; George and Qureshi, 2013):

$$\tau = \eta\gamma, \tag{17}$$

where τ is the shear stress (Pa), η is the viscosity (Pa.s) and γ is the shear rate (s^{-1}).

The behaviour of non-Newtonian fluids can be described through the power-law viscosity model, proposed by Ostwald in 1925 (Chhabra and Richardson, 1999; George and Qureshi, 2013):

$$\eta = K\gamma^{n-1}, \tag{18}$$

where K is the consistency index (Pa.s^n) and n is the flow behaviour index (dimensionless).

Depending on the value of n, different regions can be identified: i) $n < 1$: shear-thinning; ii) $n = 1$: Newtonian; and iii) $n > 1$: shear-thickening.

Ideal inks should have two properties: i) they should exhibit a shear-thinning behaviour upon the application of a deforming force; and, ii) their viscosity should increase quickly after the removal of the force to guarantee high shape fidelity and printing accuracy (Amorim et al., 2021; Ramesh et al., 2021). Most inks used for HFE 3D printing (e.g., temperature-sensitive hydrogels, partially crosslinked hydrogels, and colloidal suspensions) can be classified as non-Newtonian systems with shear-thinning properties, whose viscosity decreases with increasing shear stress.

4.1.1.2. Viscosity. Viscosity can be defined as the resistance of a fluid to flow during the application of stresses and is a major influencer of extrudability, printing accuracy and shape fidelity. In practical terms, viscosity is defined as the ratio of shear stress to shear rate. The viscosity of hydrogel inks can be influenced by: i) temperature: ii) polymer concentration; iii) molecular interactions; and, iv) molecular weight (Schwab et al., 2020). Usually, higher viscosity inks result in higher printing accuracy and can more easily retain shape after extrusion. However, an increase in viscosity requires an increase in the extrusion shear stress, which can also influence cell viability and consequent biological performance or drug retention capabilities (Cooke and Rosenzweig, 2021; Schwab et al., 2020; Shahbazi and Jäger, 2021). To avoid the need of increasing extrusion shear stress, it is also possible to control extrudability by using different nozzle geometries or sizes (see Section 4.1.2) or by adjusting printing parameters (see Section 4.2). Low viscosity hydrogel inks can minimize nozzle clogging during printing but can result in poor printing accuracy and shape fidelity retention (Mohammed et al., 2021).

4.1.1.3. Yield stress. The yield stress or yield point indicates the limit of elastic behaviour, corresponding to the minimum stress that is necessary to induce flow, and can be measured through shear stress sweep tests. Ideal inks are those with yield stress followed by a high shear effect, therefore fitting the Herschel-Bulkley equation (Amorim et al., 2021; George and Qureshi, 2013; Shahbazi and Jäger, 2021; Townsend et al., 2019). Some authors suggest that the yield stress can be considered an important parameter to infer over the printing accuracy and shape fidelity, and it can also serve as an indirect indication of the ink's ability to support subsequent stacked layers (Amorim et al., 2021). Cooke *et al.* (Cooke and Rosenzweig, 2021) also highlighted that the ink's yield

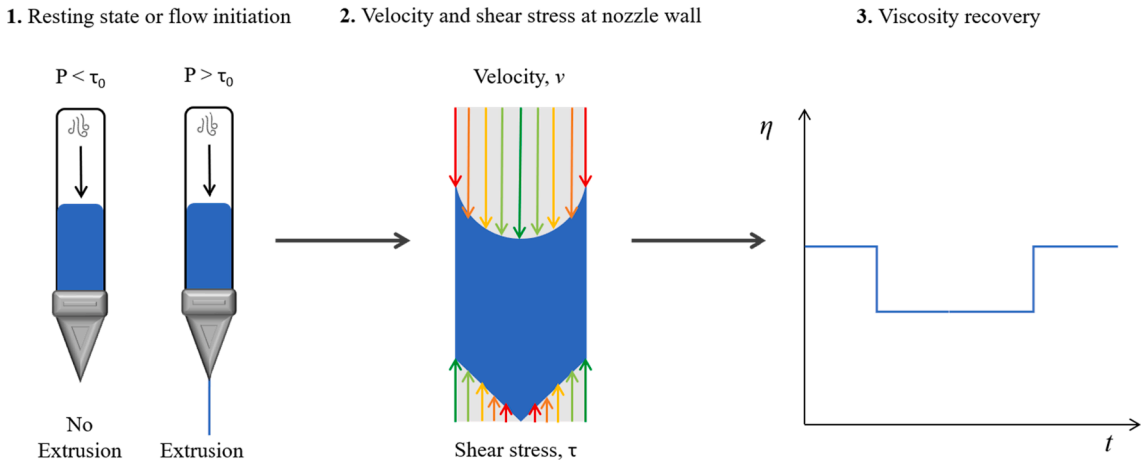

Fig. 3. Rheological parameters influencing printing. The force driving extrusion needs to be greater than the material yield stress to counteract resistance to movement. The velocity of the ink increases in the centre of the nozzle and decreases near the nozzle wall. On the opposite, shear stress is bigger next to nozzle walls and smaller near the centre. Printed materials need to recover their viscoelastic behaviour upon deformation induced by shear stress to produce 3D constructs with proper shape fidelity.

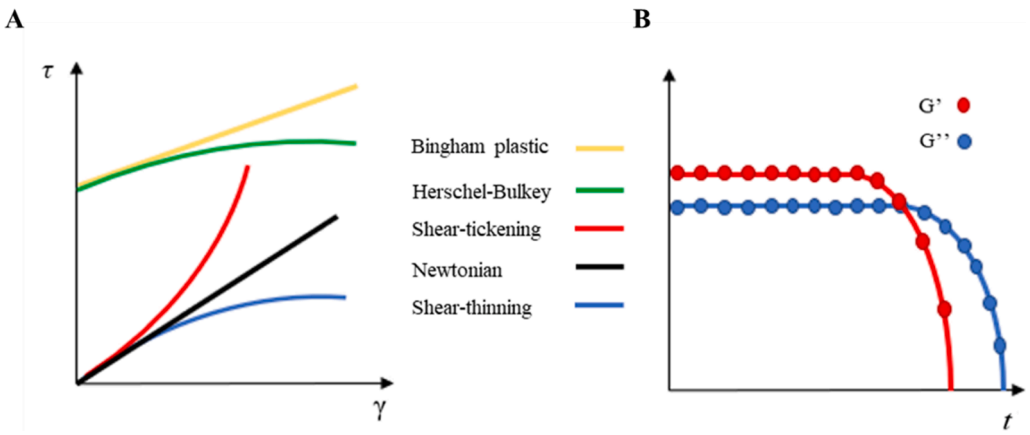

Fig. 4. Flow behaviour. (A) Relation between shear stress and shear rate in different materials, where the slope of the function is viscosity. Materials can be categorized based on the obtained curve profile. **(B)** Oscillatory frequency sweep test with controlled shear strain, showing the crossover point representing the sol-gel transition phase.

stress determination can be useful to presume the required pressure needed for extrusion. In particular, the research carried out by Mouser *et al.* (Mouser et al., 2016), showed that yield stress plays a crucial role in filament formation and deposition, suggesting that high yield stresses in which viscosity decreases rapidly result in adequate extrudability and higher printing accuracy. Ribeiro *et al.* (Ribeiro et al., 2017) further proposed a straightforward theoretical model to predict filament collapse, after printing, directly from the yield stress value, which can be of great value for optimization studies. However, Amorim *et al.* (Amorim et al., 2021) highlighted that the yield stress effect by itself is not an indicator of good printability, being necessary to analyse other parameters to infer this parameter.

4.1.1.4. Thixotropy. A three interval-time-thixotropy test can also be performed to investigate the viscosity recovery behaviour of the 3D printed structure, and the time required for that to occur; this test measures the viscosity within 3 shearing intervals: i) low shear interval (until a shear rate value of 10^0 s^{-1}) to check the viscosity of the ink before printing; ii) high shear interval to simulate the stress exerted inside the nozzle walls; and, iii) low shear interval for monitoring the recovery ability (Amorim et al., 2021; Cooke and Rosenzweig, 2021; Jiang et al., 2019; Zhang et al., 2021). However, and as highlighted by Amorim *et al.* (Amorim et al., 2021), measuring the recovery behaviour by means of oscillatory tests (shear storage modulus *vs* time) can be more helpful than by rotational tests, since the first option integrates the elastic modulus which plays an equally important role in this process. Up to date, this approach has not yet been properly explored.

4.1.1.5. Viscoelastic shear moduli. A considerable number of reported studies only analyse viscosity (through rotational tests) as a measure of the influence of ink components, and ultimately to select the optimal formulation(s) for advancing the research. However, oscillatory tests should also be considered to characterize the viscoelastic features of hydrogel inks, by determining the loss or viscous modulus (G“) and the storage or elastic modulus (G’). In the context of HFE 3D printing, G” is used to describe the viscous flow (representing the phenomenon of ink passing through a nozzle) and G’ is linked with the elastic component that influences the printing accuracy and determines the shape fidelity (after printing) (Amorim et al., 2021). A proper balance between viscous and elastic modulus is required to guarantee high printing accuracy and shape fidelity, as highlighted by Townsend *et al.* (Townsend et al., 2019). Usually, these complex moduli are measured through amplitude or frequency sweep tests with controlled shear strain. The first one is normally used to determine the linear viscoelastic region (LVER) and to define the shear strain to be used in the frequency sweep test. The second test, in addition to being able to characterize the viscoelastic behaviour of the hydrogel inks within the LVER, also makes possible to determine the yield stress. In addition to these assays, a single frequency strain-controlled time event sequence or a single frequency strain-controlled ramp test can be used to assess the time- and temperature-dependent viscoelastic behaviour, respectively (Fig. 4(B)) (Amorim et al., 2021; Cooke and Rosenzweig, 2021). Furthermore, it is also highly recommended to determine the loss or damping factor, Tan δ (G“/G’), which describes the viscoelastic behaviour through a dimensionless index in samples when there is a phase transition (sol-gel phase) (Bom et al., 2020; Gao et al., 2019; Seoane-Viaño et al., 2021).

In a previous report by our group (Bom et al., 2020), it is highlighted that Tan δ (G“/G’) can be presented as a function of time sequence, which allows the determination of gelation time for ionic-crosslinked hydrogel inks in function of the viscoelastic behaviour by defining the crossover point. Furthermore, these data were also used to infer over the adhesiveness strength of the hydrogel inks developed. A single frequency strain controlled with temperature ramp test can also be performed to determine gelation time and the printing temperature range interval (PTRI) for physical or UV crosslinked hydrogel inks (Amorim et al., 2021). According to O’Connell *et al.* (O’Connell et al., 2017), special care must be taken when selecting the ramp rate (°C/min), since it is necessary to assure that the sample tracks the temperature of the measuring system, avoiding sudden changes in temperature. According to the same authors, the ramp rate should not exceed 2 °C/min.

Gao *et al.* (Gao et al., 2019) studied the effect of G’, G“ and Tan δ on the printing accuracy in z-axis (defined as structural integrity) and printing precision (referred to as extrusion uniformity) using alginate/gelatin-based inks (studied as single polymeric components and as a mixture). In addition, a first-order interactive model was established to correlate G’ and G” with the extrudability pressure. Lower Tan δ was correlated with increased printing accuracy in z-axis, whereas higher Tan δ was correlated with increased printing precision. The results further showed that the extrusion pressure of a hydrogel ink is co-determined by G′ and G″, highlighting the influence of the ink elastic properties. Although these results may not reflect all polymeric materials that can be used as extrusion printing inks (only two model materials have been studied), they certainly indicate the proper methodology to be used when evaluating the printing quality of other hydrogel inks whilst considering their viscoelastic behaviour. This study also showed that, although viscosity can be considered the primary physicochemical parameter affecting print quality, by itself it does not reflect the complex behaviour of hydrogel-based inks during the 3D printing process.

Park *et al.* (Park et al., 2020) established rheological methods to study the effects of cooling and heating rates on sol-gel and gel–sol transitions. The authors performed temperature sweep tests with

oscillatory shear, using gelatin methacryloyl as a representative compound, at four rates: 0.3 °C/min, 0.6 °C/min, 2.5 °C/min, and 10 °C/min. The results highlighted that the higher cooling rates led to lower temperatures at which the increases in G′ and G″ occurred, and to lower gelation temperatures; effects like this were also noticed for the heating assays performed, although less significantly. Furthermore, the authors emphasized that the cooling/heating mechanism of the rheometer by a Peltier bottom plate increased these effects, since only the bottom of the sampl-es was cooled down or heated. Overall, these results suggest that temperature sweep tests must be performed at several rates, or that the rate should be identified as relevant to the actual application, in order to be representative of the physical gelation process under evaluation.

4.1.2. Nozzle selection

Selecting a nozzle tip is a pivotal component of the pre-printing optimization process, as it can have a considerable effect on determining the optimal printing speed and pressure, as well as on achieving adequate extrudability, printing accuracy and shape fidelity. Within this context it is necessary to consider the nozzle inner diameter, length, profile, geometry, and material. As a rule, the extrudability of hydrogel inks increases when: i) the diameter of the nozzle is larger; ii) the nozzle length is shorter; and, iii) conical nozzles are used instead of cylindrical nozzles (Gillispie et al., 2020). On the contrary, printing accuracy and shape fidelity increase when the inner diameter of the nozzle is smaller (Bom et al., 2020; Webb and Doyle, 2017). However, the probability of partial or full nozzle clogging increases proportionally with the decrease in the nozzle inner diameter, which in turn is related with the viscosity properties of the hydrogel ink. Partial nozzle clogging can cause geometric misalignments by dragging material during printing, as well as leading to the extrusion of a smaller amount of material, which in turn can affect printing accuracy and precision. Full nozzle clogging requires cleaning the cartridge and nozzle, delaying the printing process. The geometry of the nozzle (e.g., conical, or cylindrical) determines the shear stress that hydrogel inks undergo during extrusion, which directly correlates with the amount of material extruded. Considering the nozzle profile, cylindrical needles require higher pressure and can be more prone to clogging, whereas tapered needles can significantly decrease the pressure needed to extrude and reduce clogging (Mohammed et al., 2021). Regarding the material, the choice should always be dependent on the extrusion temperature and/or formulation components. The choice of the ideal nozzle is characterized by such trade-offs, making this a fundamental step in the optimization process.

Cai *et al.* (Cai et al., 2020) reported a study testing two different nozzles: the precision stainless steel tip (cylindrical shape with inner diameter of 250 μm), and the smooth flow tapered tip (conical shape with inner diameter of 250 μm). The results showed that when the cylindrical nozzle was used, thinner and straighter filaments were obtained compared to those printed with the conical nozzle (although the diameter of the nozzles was the same). However, when using the cylindrical nozzle, a higher printing pressure was required, possibly because this nozzle has a longer narrow tip end. Overall, the results suggested that cylindrical nozzles afford a higher printing accuracy and shape fidelity, compared to conical nozzles.

Magalhães *et al.* (Magalhães et al., 2019) resorted to computational fluid dynamics (CFD) simulations to evaluate the shear stress caused by the internal pressure of different nozzle designs, varying convergence angles, needle hub lengths, shaft lengths, and exit diameters; the inlet diameter was fixed as 10 mm for all nozzles. The data obtained showed that small convergence angles at the shaft, lead to higher nozzle walls shear stresses, and bigger exit diameters worst the printing accuracy. Overall, convergence angles and exit diameters were disclosed as the most important parameters that affect the balance between shear stress and printing resolution.

4.1.3. Correlation between rheology and nozzle selection: Influence on printing

To identify the optimal printing parameters, besides rheological features, it is also necessary to consider geometrical (nozzle) and instrumental (printer) parameters. For example, the optimal range of rheological properties for a hydrogel ink to be printed at 45 °C and 20 PSI through a conical nozzle with 100 μm, will be different when considering a higher nozzle inner diameter or a cylindrical nozzle; the same is true if the pressure is changed. Thus, some authors have described the potential of using mechanical fluid model laws to derive the flow rate, since it is a readily quantifiable measure of extrusion. For extrusion 3D printing, the flow rate is influenced by the ink flow behaviour, temperature, nozzle geometry, and dispensing force. Jiang *et al.* (Jiang et al., 2019) listed all the common mathematical equations that can be used to model extrusion for both cylindrical and conical nozzles and discussed their potential contribution to the development of complex and accurate extrusion models, while several other authors have been focusing on the development and application of such complex models. For example, Chen *et al.* (Sarker and Chen, 2017) developed a model based on the fundamentals of fluid mechanics to evaluate the flow rate of chitosan-based inks using a modified pneumatic-dispensing 3D printer. The model included pressure, temperature, needle geometry, surface tension and rheological parameters, and the authors emphasized the influence of the needle geometry and yield stress features of the hydrogel inks on the determination of the flow rate. Kang *et al.* (Kang et al., 2013) used the Hagen-Poiseuille law to describe the fluid flow and approximate the maximum wall shear stress in the nozzle based on pressure, nozzle diameter and hydrogel viscosity. A study by Sarker *et al.* (Sarker and Chen, 2017) focused on the development of model equations based on mechanical fluid model laws to predict the flow rate of alginate hydrogel inks with varying concentrations (1–4%) and at different temperatures (25–55 °C), considering the shear and slip flow from a tapered needle.

4.2. Printing

To adequately assess the potential that a particular ink has to create constructs with high resemblance to the computer-aided design (CAD), in a reproducible way, the parameters which are related to the design and the printer machine should be adjusted.

4.2.1. Design

The construct's design is the primary step to guarantee the printing quality, namely in the design of complex and intricate structures. CAD models, which are the conceptual drawings of a structure to be mimicked by the printer in a plane with (x,y,z) coordinates, are generally built-in specialized softwares. There are several CAD programs commercially available, and some are free online. However, the sensitivity of ink formulations further hinders the establishment of optimized CAD simulations (O'Connell et al., 2017; Ramesh et al., 2021). Computed Tomography (CT) scans and magnetic resonance imaging (MRI) have demonstrated potential to accelerate this process, since these are able to adequately delimit the outlines of tissue constructs at a faster pace (Datta et al., 2018; Peng et al., 2017; Unagolla and Jayasuriya, 2020; Wang et al., 2015).

After creating a 3D model from one of the methods mentioned above, an .stl file is created and imported into a slicing software (e.g., Cura, Slic3r, and RepSnapper). Slicing is the automated creation of G-code based on the submitted CAD model, i.e., it cuts the 3D model into cross-sectional layers and establishes the commands that the printer must meet to print each layer. Generally, layer width and height are user-set parameters that will modulate the slicing procedure (Baumann et al., 2016). This type of software also offers the possibility of simulating and printing support regions, i.e., regions that do not compose the 3D model originally, but that must be created to support the formation of other parts which are effectively represented in the 3D model. In the end of the

process, a G-code file is generated that contains the full set of commands to which the printer will conform so that the desired construct is produced. Understanding G-code is not crucial to have successful prints, but it is useful to the printer user because it allows to manipulate both the structure and printing process post-slicing, offers flexibility in troubleshooting, and can accelerate some printing procedures. Nevertheless, the variation that exists between commercially available printers, regarding the accepted G-code, somewhat hinders a standardized knowledge of the latter.

4.2.2. Printer

Some parameters of the process must be defined by the operator to the equipment, namely: Pressure (P) - the driving force of extrusion in pneumatic-based systems, where different flow rates originate at different pressures; Nozzle offset (NO) - the distance between the nozzle and the printing bed; Feed rate (F) - also named as nozzle speed or velocity, it corresponds to the moving speed of the printer's arm and nozzle; Temperature (T) - the temperature of the ink inside the cartridge; and, Nozzle geometry (NG) - embraces sub parameters such as nozzle diameter, nozzle length and type of nozzle.

However, the optimal values for these user-set parameters are generally unknown. The aforementioned rheological analysis enables researchers to predict a temperature range for printing or the minimum required pressure for extrusion, for instance, but these are insufficient to deliver the most accurate printing. Therefore, it is necessary to adjust such parameters to the ink in use, and the tests displayed below aim at providing the narrowest group of parameter settings possible.

4.2.3. Optimization of parameters related to extrudability

4.2.3.1. Filament drop test. An adequate extrudability is fundamental to have an optimal printing process. Therefore, it is necessary to optimize extrusion-related parameters, with pressure being the most relevance in pneumatic HFE (He et al., 2016; Naghieh and Chen, 2021). First and foremost, the pressure exerted to extrude material has to be higher than the material surface tension and/or yield stress (He et al., 2016; Naghieh and Chen, 2021; Schwab et al., 2020), otherwise there will be no extrusion due to the resistance to flow of the ink.

He *et al.* (He et al., 2016) suggested a test of static extrusion in which sodium alginate would be extruded at different pressures and temperatures, in order to assess the size of hanged filaments. However, the criteria for choosing an optimal size range are poorly defined and greatly depend on the viscosity of the materials being used. Other authors have added that this type of test also gives detail about the gelation status and homogeneity of the ink (Cai et al., 2020; Habib et al., 2018; Ouyang et al., 2016; Paxton et al., 2018; Suo et al., 2021; Wu et al., 2018). Specifically, inks are generally classified as under-gelled, if a droplet forms at the nozzle tip, properly gelled if a continuous filament is extruded (Cai et al., 2020; Habib et al., 2018; Ouyang et al., 2016; Paxton et al., 2018; Wu et al., 2018), or over-gelled if an irregular, curvy and non-uniform filament is formed (Fig. 5(A)) (Cai et al., 2020; Ouyang et al., 2016; Wu et al., 2018). Thus, this test is useful to verify if the sol-gel transition temperature defined by rheological analysis is correct. However, droplets can form with over-gelled formulations, and a continuous filament may not accurately translate into a properly gelled solution, since under-gelled formulations can also depict similar behaviour and, in addition, cause jet-like extrusion, if pressures are high enough. Indeed, it has been shown that alginate inks with increasing concentrations of $CaCl_2$, which are relatively close to an over-gelled status, could form droplets that can achieve higher printing accuracies when printing grid-like structures compared to inks that form continuous filaments (Kim et al., 2019; Park et al., 2017). Because the mechanism of HFE is directed to printing on solid surfaces, rather than into air, which creates the need of validating this test with effective filament printing, we believe that tests that use deposition are preferable for determination of extrudability parameters.

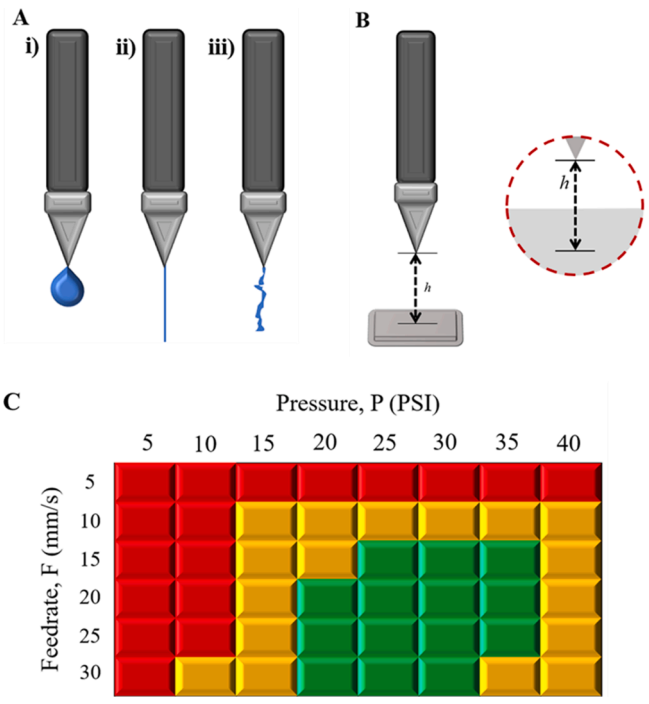

Fig. 5. Optimization of parameters related to extrudability. **(A)** The filament drop test has 3 outcomes regarding the filament shape after extrusion, depending on the used materials and printing parameters: (i) droplets, (ii) continuous filaments, or (iii) bumpy and irregular filaments. **(B)** Delimiting an ideal nozzle offset is vital to an accurate printing. **(C)** Hypothetical representation of a process map for the optimization of pressure and feed rate in which the window of optimal parameters is defined by measurements of the spreading ratio.

4.2.3.2. Nozzle offset test. Nozzle offset, which represents the distance between the nozzle and the printing surface, is often considered since it can affect the printing accuracy and shape fidelity of 3D constructs (Fig. 5(B)). Furthermore, this parameter should be carefully defined and precisely controlled over the experiments to guarantee high printing precision (Mohammed et al., 2021; Naghieh and Chen, 2021; Schwab et al., 2020). Naghieh *et al.* (Naghieh et al., 2019) evaluated the influence of nozzle offset in the line width at a constant nozzle speed of 35 mm/s, using a 200 μm nozzle. By modulating the nozzle offset, a wide range of strand diameters were obtained, varying from 0.1 to 0.6 mm, which reinforces the importance of adjusting such printing parameters. The authors further highlighted that a large nozzle offset can lead to non-continuous printing, while a small distance between the printing surface and the nozzle may lead to squeezing of the ink or hinder the proper ink flow during deposition.

4.2.3.3. Linear filament tests. Due to the limitations mentioned for the test above, to the lack of a rheological model that allows the prediction of an ideal pressure, and to the shortage of tests that allow varying the pressure while keeping all other parameters constant, the extrusion pressure needs to be defined using other approaches. Printing simple linear filaments with a constant width (which can be defined in the slicing software) is a method of deposition that permits the assessment of the optimal pressure and feed rate. Recently, Armstrong *et al.* (Armstrong et al., 2021) applied a method to qualitatively categorize extrudability by evaluating line width, with the creation of a 'process map', in which filaments with smaller spreading delimit a range of optimal extrusion parameters (Fig. 5(C)). The authors went further and defined material models which are implemented into controlled designs

that contain varying parameters while printing, thus delivering superior constructs. Some printers, however, may not possess this ability. Nozzle offset and temperature are parameters that can be used to represent a third dimension which could possibly be incorporated into this mapping procedure. The spreading ratio is a way of analysing line width and is typically quantified by measuring printed lines with imaging software and fitting equation (19) to the obtained values:

$$Spreadingratio = \frac{Printedneedlediameter}{Needlediameter} \quad (19)$$

Therefore, spreading ratios closer to 1 translate into excellent printing because measured and defined line widths are similar (Ramesh et al., 2021). Increasing feed rates will, up to a certain point (which is dependable on the ink), deliver narrower filaments, and slower feed rates will return thicker filaments due to material accumulation (He et al., 2016).

4.2.4. Characterization of printed hydrogels

Once the adequate window of printing parameters for a given ink is determined, the characterization of several printed constructs which differ both in morphology and layer number, must be performed. This characterization allows to further narrow the set of printing parameters and, more importantly, to assess if the formulation is capable of rendering high quality and complex 3D structures.

4.2.4.1. Filament fusion tests. Filament fusion tests consist in printing a meandering pattern with parallel strands and decreased spacing between filament segments, so that the merging between these can be evaluated (Cai et al., 2020; Ribeiro et al., 2017; Schwab et al., 2020). Therefore, it is possible to establish the minimum distance necessary to avoid filament merging, for a particular set of parameters. After deposition, the material is prone to spread and merge due to the surface tension between ink and support adhesion materials (e.g., plastic, glass, others) and between adjacent filament segments, leading to a time-dependent loss of resolution (Cai et al., 2020; Schwab et al., 2020). Lower material spreading and fusion results in higher printing resolutions, since the distance needed to create two distinct parallel filaments is lower. Inks with lower yield stress or under-gelled tend to have larger propagation of fused segments. Consequently, the initial filament distance should consider the ink rheological features and nozzle diameter. Ribeiro *et al.* (Ribeiro et al., 2017) applied, in a composite ink of poloxamer and PEG, an initial distance of 0.25 mm, with a gap increase of 0.05 mm *per* line, up to a distance of 0.55 mm. Cai *et al.* (Cai et al., 2020) reversed the direction of the test by moving through decreased spacing, in distances ranging from 2 mm to 0.5 mm in alginate-gelatin formulations that incorporated laponite. The design of the meandering pattern should consider the following parameters to better assess shape fidelity and printing accuracy (Fig. 6(A)): (1) f_s – fused segment length; (2) f_d – filament distance; (3) f_t – filament thickness. These are quantifiable through imaging software, but visual inspection may be sufficient if simpler constructs are to be designed. The f_s parameter tends to increase with decreasing f_d, creating an exponential function in which the effect of f_t is addressed by normalizing f_s with the average f_t. Regarding the number of layers, it can be done in single layers, although the use of 3 or more layers is also informative. For instance, Habib *et al.* (Habib et al., 2018) designed a 4-layered meandering pattern with a distance range of 1–5 mm in 1 mm increments of filament spacing, where subjacent layers were in 0°-90° rotational patterns.

4.2.4.2. Filament collapse test. The collapse test offers insight over the structural stability of the material, which is one of the requisites of shape fidelity. It is important that the hydrogel can counteract its own weight and gravity deformation, since multi-layered constructs will often have shapes with overhangs or parts with filaments that contain no underlying support. The test is performed on top of a structure that contains pillars with increasing distance. Analysis is conducted through the measurement of the angle of deflection (Fig. 6(B)), which indicates the degree of collapse (Cai et al., 2020; Kim et al., 2018; Ribeiro et al., 2017; Schwab et al., 2020). The angle of deflection can be measured by utilizing 20 s video stills, as proposed by Ribeiro *et al.* (Ribeiro et al., 2017), whereas other authors used imaging software at both defined (Kim and

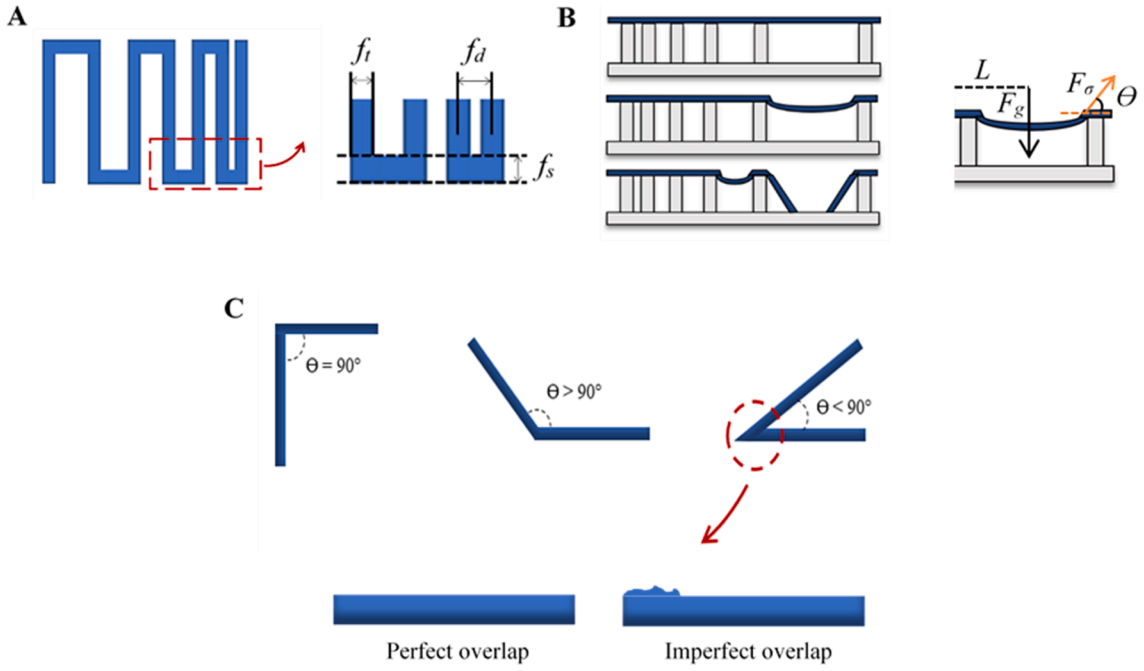

Fig. 6. Characterization of printed hydrogels. (A) Meandering pattern used for fusion tests; f_s - fused segment length, f_t - filament thickness, f_d - filament distance. **(B)** Depiction of possible outcomes in filament collapse tests, with and without sagging; L - length, F_g - gravitational force, Θ - deflection angle, F_σ - force exerted by the filament to counteract gravity. **(C)** Angle printing (right, obtuse, and acute/sharp angles) allows the assessment of overlapping in regions where the direction changes abruptly.

Nam, 2020) and undefined time frames (Cai et al., 2020). Naturally, smaller angles of deflection translate into more stable structures, as is the case of materials with higher yield stress, hence it is assumed that inks with low yield stress will generate high deflection angles or even break and collapse (Ribeiro et al., 2017; Schwab et al., 2020). However, this type of materials can still have their angle of deflection analysed in the smaller gaps. Another method, proposed by Habib *et al.* (Habib and Khoda, 2018), suggests that a collapse area factor (Cf) can also be used to analyse deflection, whilst resorting to the theoretical (At) and actual (Aa) area between the two pillars (equation (20)):

$$Cf = \frac{At - Aa}{At} x100\% \quad (20)$$

Materials which are unable to bridge the gap between pillars will have a collapse factor equal to 0, whilst a straight filament will have a collapse factor of 100% (Habib et al., 2018; Habib and Khoda, 2018).

Perhaps the major drawback of this test is that the pillar array structure is not commercially available, which conjectures some variability regarding gap dimensions, with gap sizes from 1 to 12 and 1 to 16 mm being reported (Cai et al., 2020; Kim and Nam, 2020; Ribeiro et al., 2017; Schwab et al., 2020; Therriault et al., 2007). The addition of more layers adds more weight for the printed filament to sustain, which could also hamper results for the deflection angle and relationships that could be extrapolated regarding yield stress.

4.2.4.3. Angle tests. Shape fidelity in angles is harder to achieve relatively to straight lines and to circles, although the latter can also present challenges to some printers, due to the sudden change of direction (Wu et al., 2018). The overlap that exists when printing sharp angles is a major concern in printing, since it can lead to printing failure due to the inability of the construct to maintain a uniform height. As will be discussed, although this test can be integrated when testing the pentagram geometry, it is recommended that the extent of the overlap problem is addressed before printing more complex structures (He et al., 2016). Generally, acute angles present the worst outcomes in overlapping terms, but obtuse and right angles should be tested as well, to gain further insight about the hydrogel potential (Fig. 6 (C)). Wu *et al.* (Wu et al., 2018) proposed a deviation rate calculated by dividing the difference between theoretical and effective angles for the theoretical angle, with sharp angles delivering higher deviation rates than obtuse angles. To minimize the overlap effects, reducing pressure/flow rate or accelerating printing speed before reaching these angles, has been suggested to improve the printing quality and thus, shape fidelity (He et al., 2016). However, not all printers possess the capability of dynamically changing pressure throughout the procedure.

4.2.5. Planar and multi-layered structures

Planar 3D constructs are sometimes preferable to more complex structures. These are typically single layered constructs and, if designed accordingly, can complement tests done previously, in addition to the assessment that can be made regarding the correct display of spatial location and size of the construct in relation to the CAD model. For these tests, the suggested geometries typically involve grids, circles, squares, and star-shaped pentagrams – Fig. 7. For instance, printing circles will check arc motion capabilities, squares are useful for quantification of printing accuracy (Koch et al., 2020), pentagrams can be used to replace angle tests, and using different infills in grid-like structures can help validate if some shapes are reproducible inside contours. Still, in single layer structures, it is possible to create complex shapes by recurring to infill patterns that can simultaneously assess printing accuracy and shape fidelity.

Nonetheless, the adequate formation of multi-layered structures is vital and might be the ultimate challenge to some inks since constructs of interest to drug delivery and tissue engineering applications will rarely consist of single layered structures. Indeed, the shapes required for tissue engineering are more intricate and complex because these often try to replicate organs or tissues. However, drug delivery applications based on printing may also aim at creating multi-layered constructs, such as patches for topical drug administration or the creation of cylindrical pills. Therefore, attempting to produce structures of several layers prior to printing complex scaffold morphologies is imperative. Moreover, it allows to assess layer stacking and, consequently, fusion height. The phenomenon of fusion between subjacent layers causes a differential between the height of printed scaffolds and the theoretical height of the CAD model, which, similarly, to overlapping, creates non-uniform heights along the construct that can cause print failure. Fusion height has been quantified by comparing effective and theoretical heights, but there is a lack of methods to visualize the deformation that spreading and consequent fusion between stacked layers cause on the filament geometry.

Grid-like structures are by far the most attempted design in hydrogel characterization (Cui et al., 2020; Jessop et al., 2019; Leucht et al., 2020; Liu et al., 2019, 2017; Wang et al., 2018), due to the formation of a matrix with transversal porosity, which fulfils the needs of scaffolds for tissue engineering in terms of providing adequate environments for cell proliferation and nutrient circulation, whilst creating biodegradable drug carriers with tunable pore size for either fast or controlled drug release for delivery applications. These structures are versatile because

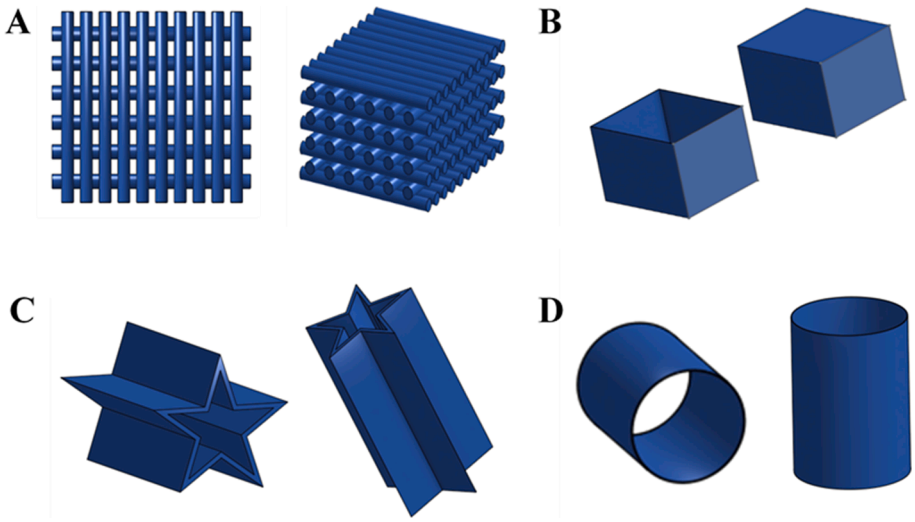

Fig. 7. Representative CAD models for (A) grid-like structures, **(B)** hollow and filled cubes, **(C)** star-shaped pentagram, and **(D)** cylinders.

they permit the characterization of different parameters, either related to the printer or to the printing process, such as the maintenance of a constant diameter in linear filaments, resistance to collapse in overhangs and parts with no subjacent support, the fusion between filaments if the pore size is relatively small, the diffusion of material in Dumbbell bars and corners, and allow the incorporation of area measurements that quantify printing accuracy. Depending on the type of infill pattern, the capability of successfully overlapping can also be studied, as well as lateral porosity (Ribeiro et al., 2017). The formation of a perfect grid-like structure means that the optimization of printing parameters was done correctly and that a particular ink is a promising candidate to be used in the printing of complex constructs. However, some inks do not possess the necessary mechanical properties to create this type of structure, even if they can be used for other types of structures. Printing multi-layered cylinders is also common practice due to the interest in bioprinting human cannular tissue (Gao et al., 2019; Jessop et al., 2019; Jia et al., 2016; Leucht et al., 2020; Liu et al., 2019, 2017; Pi et al., 2018) and it can address the problem that some printers have in delivering the same resolution when printing in arc motions. Additionally, it is a type of structure of simple design that facilitates the measurement of fusion height and the maintenance of shape fidelity over time, something that is feasible right after printing as well as several hours or days later (Jessop et al., 2019). Pi *et al.* (Pi et al., 2018) were able to bioprint hollow cylinders with an inner and outer layer composed of different materials that aim at mimicking native tubular tissue. Liu *et al.* (Liu et al., 2019) combined both hollow cylinders, also constituted by different materials, and grids, by printing lattice structures with hollow fibers, similarly to the work reported by Kim *et al.* (Kim and Nam, 2020). The same rationale of measuring fusion height can be applied regarding printing hollow cubes, but these are often neglected since the information obtained with these structures can also be obtained with cylindrical structures. Still, the overlap influence of right angles over fusion height is determinable. Filled cubes have been printed to assess shape fidelity (Liu et al., 2017) and have been attempted as patches for topical drug delivery (Bom et al., 2021, 2020). Printing multi-layered star-shaped pentagrams, besides allowing to check shape fidelity, printing accuracy and height uniformity in apexes and edges, also corroborate the results of previous angle tests that regard overlap impact.

5. Conclusions and future outlook

The pharmaceutical, cosmetic, and (bio)medical research communities have been studying the possibility of using hydrogel extrusion 3D printing to fine-tune drug delivery rates by varying the extent of cross-linking, the polymeric material used, and/or the design of the 3D construct, to substitute conventional pills and tablets that offer fixed dosages (Lee et al., 2019). One of the exciting future directions in the fields of 3D technology is indeed the print of new personalized smart constructions for bio-applications. These constructions can perform specific functions, such as disease treatment or increase the normal capabilities of the human body. The production of smart constructions by 3D printing is already a reality, but there is still a long way to overcome the limitations of the 3D printing process, which includes the development of inks with new compositions, adequate rheological properties, and improvement of printing resolution to guarantee high printing accuracy and fidelity.

3D (bio)printing is still in its beginning, , therefore it is not surprising that both nomenclature and procedures are not yet properly standardized.. Herein, we propose the adoption of only five concepts, namely printability, extrudability, printing accuracy, shape fidelity, and printing precision, which translate the essentials that must be considered in a hydrogel-forming extrusion (HFE) -based 3D printing process. The adoption of less but concise concepts is proposed as a way of simplifying and grouping concepts that were previously divided, thus avoiding the current lack of uniformity found in the literature. Another important aspect that must be highlighted is that the concept of printability must be seen as the result of all others and cannot be limited to just one measure of characterization. In this context, it is also necessary that researchers start considering the adoption of hydrogel inks characterization protocols that should include both pre-printing (rheology and nozzle selection) and printing assays. Few researchers consider rheology as a valuable tool, and most only routinely use rotational viscosity tests, disregarding the evaluation of the elastic properties, which have an equally significant impact on parameters such as extrudability, printing accuracy and shape fidelity. Furthermore, and as previously mentioned by Cooke *et al.* (Cooke and Rosenzweig, 2021), new rheological sequences can be designed by combining the analysis of different parameters that are usually characterized separately, to replicate the printing process and environmental conditions. Thus, it is expected that, soon, different and more robust rheological tests will be included in the characterization and optimization protocols of hydrogel inks.

Since rheological parameters are the major influencers for successful printing procedures, the methods used for downstream optimization of printing parameters or for the ink characterization should consider both the material and printing mechanism utilized (Lee et al., 2020; Pati et al., 2015). For instance, if the ink has a high viscosity and the operator is free to choose between a pneumatic or a screw-driven extrusion, the latter would be a wiser choice considering the rheology of the formulation (Pati et al., 2015). As discussed, pressure remains the most relevant printing parameter in pneumatic extrusion, but methods to adequately define it whilst other parameters are kept constant are still lacking. The considerations withdrawn from the filament drop test seem very dependent on the ink composition and profile, which can lead to different researchers defining different pressure ranges as optimal for the same material. The idea of a process map is an alternative where other parameters are not constant, something that can cause variance across studies as well, in addition to being relatively slow. The filament fusion test and the filament collapse test both offer quantitative parameters, such as the angle of deflection or the fused segment length, allowing researchers to predict the potential use of a previously studied hydrogel in a particular application. Regarding planar and multi-layered structures, it would be ideal if standard shapes were constantly applied and reported throughout different studies for comparison and reproducibility. Still, the use of different infill patterns, which can create more complex shapes, is recommended if researchers aim at further characterizing a specific formulation. In addition, and although the determination of fusion height during layer stacking is tackled by measuring and comparing both the CAD model and construct height, there is still no method that allows to assess which regions of the filament are being morphologically affected by the merging and/or spreading of the different layers, which may represent a problem when fabricating more complex shapes.

For the sake of progress and to accelerate the implementation of this technology, it is imperative that methodologies employed by different research groups become standardized and universal, thus sharing common features. This would allow to characterize several inks in a simultaneously fast and practical manner, which would grant a correct comparison of formulations developed. This is also of major interest because it will further clarify, both in the technical and regulatory standpoint, the potential of a hydrogel ink to be used, e.g., on tissue engineering or drug delivery. As previously mentioned by our group (Bom et al., 2021), it is expected that new regulatory guidelines emerge soon, and the clarification and adoption of such standardized methodologies for optimization and characterization of hydrogel inks represent a great advance, particularly in terms of product safety and quality, to guarantee the widespread use in pharmaceutical and medical contexts. Furthermore, the adoption of such methods could serve to eventually create a public database regarding the performance and printability of the various polymers available for HFE, allowing a faster implementation of this type of manufacturing technologies in industrial, pharmaceutical and hospital environments, and subsequently facilitate the customization of the 3D printed vehicles.

Funding

This research was funded by the Fundação para a Ciência e Tecnologia, Portugal (UIDB/04138/2020 and UIDP/04138/2020 to iMed. ULisboa, PTDC/MEC-DER/30198/2017 and CEECINST/00145/2018 to J.Marto, and CQE UIDB/QUI/00100/2020 to C.Santos. S.Bom was supported by a PhD fellowship (3DGelComp project) from Instituto Politécnico de Setubal.

CRediT authorship contribution statement

Sara Bom: Conceptualization, Writing – original draft. **Ricardo Ribeiro:** Conceptualization, Writing – original draft. **Helena M. Ribeiro:** Writing – review & editing, Project administration. **Catarina Santos:** Conceptualization, Writing – review & editing, Supervision, Project administration. **Joana Marto:** Conceptualization, Writing – review & editing, Supervision.

Declaration of Competing Interest

The authors declare that they have no known competing financial interests or personal relationships that could have appeared to influence the work reported in this paper.

References

Agarwal, T., Banerjee, D., Konwarh, R., Esworthy, T., Kumari, J., Onesto, V., Das, P., Lee, B.H., Wagener, F.A.D.T.G., Makvandi, P., Mattoli, V., Ghosh, S.K., Maiti, T.K., Zhang, L.G., Ozbolat, I.T., 2021. Recent advances in bioprinting technologies for engineering hepatic tissue. Mater. Sci. Eng. C 123, 112013. https://doi.org/10.1016/j.msec.2021.112013.

Amorim, P.A., D'Ávila, M.A., Anand, R., Moldenaers, P., Van Puyvelde, P., Bloemen, V., 2021. Insights on shear rheology of inks for extrusion-based 3D bioprinting. Bioprinting 22, 1–13. https://doi.org/10.1016/j.bprint.2021.e00129.

Armstrong, A.A., Pfeil, A., Alleyne, A.G., Wagoner Johnson, A.J., 2021. Process monitoring and control strategies in extrusion-based bioprinting to fabricate spatially graded structures. Bioprinting 21, 1–10. https://doi.org/10.1016/j.bprint.2020.e00126.

Azad, M.A., Olawuni, D., Kimbell, G., Badruddoza, A.Z.M., Hossain, M.S., Sultana, T., 2020. Polymers for extrusion-based 3D printing of pharmaceuticals: A holistic materials–process perspective. Pharmaceutics 12, 1–34. https://doi.org/10.3390/pharmaceutics12020124.

Baumann, F., Bugdayci, H., Grunert, J., Keller, F., Roller, D., 2016. Influence of slicing tools on quality of 3D printed parts. Comput. Aided. Des. Appl. 13 (1), 14–31. https://doi.org/10.1080/16864360.2015.1059184.

Bedir, T., Ulag, S., Ustundag, C.B., Gunduz, O., 2020. 3D bioprinting applications in neural tissue engineering for spinal cord injury repair. Mater. Sci. Eng. C 110, 110741. https://doi.org/10.1016/j.msec.2020.110741.

Bom, S., Martins, A.M., Ribeiro, H.M., Marto, J., 2021. Diving into 3D (bio)printing: A revolutionary tool to customize the production of drug and cell-based systems for skin delivery. Int. J. Pharm. 605, 1–20. https://doi.org/10.1016/j.ijpharm.2021.120794.

Bom, S., Santos, C., Barros, R., Martins, A.M., Paradiso, P., Cláudio, R., Pinto, P.C., Ribeiro, H.M., Marto, J., 2020. Effects of starch incorporation on the physicochemical properties and release kinetics of alginate-based 3D hydrogel patches for topical delivery. Pharmaceutics 12, 1–20. https://doi.org/10.3390/pharmaceutics12080719.

Boularaoui, S., Al Hussein, G., Khan, K.A., Christoforou, N., Stefanini, C., 2020. An overview of extrusion-based bioprinting with a focus on induced shear stress and its effect on cell viability. Bioprinting 20, 1–17. https://doi.org/10.1016/j.bprint.2020.e00093.

Cai, F.F., Heid, S., Boccaccini, A.R., 2020. Potential of laponite incorporated oxidized alginate–gelatin (ADA-GEL) composite hydrogels for extrusion-based 3D printing. J. Biomed. Mater. Res. - Part B Appl. Biomater. 109, 1–15. https://doi.org/10.1002/jbm.b.34771.

Carrow, J.K., Kerativitayanan, P., Jaiswal, M.K., Lokhande, G., Gaharwar, A.K., 2015. Polymers for Bioprinting. In: Atala, A., Yoo, J.J. (Eds.), Essentials of 3D Biofabrication and Translation. Elsevier Inc., pp. 229–248 https://doi.org/10.1016/B978-0-12-800972-7/00013-X.

Chhabra, R.P., Richardson, J.F., 1999. Non-Newtonian Flow in the Process Industries. Butterworth Heinemann, Oxford.

Cooke, M.E., Rosenzweig, D.H., 2021. The rheology of direct and suspended extrusion bioprinting. APL Bioeng. 5, 1–21. https://doi.org/10.1063/5.0031475.

Cui, X., Li, J., Hartanto, Y., Durham, M., Tang, J., Zhang, H.u., Hooper, G., Lim, K., Woodfield, T., 2020. Advances in Extrusion 3D Bioprinting: A Focus on Multicomponent Hydrogel-Based Bioinks. Adv. Healthc. Mater. 9 (15), 1901648. https://doi.org/10.1002/adhm.v9.1510.1002/adhm.201901648.

Curti, F., Drăguşin, D.M., Serafim, A., Iovu, H., Stancu, I.C., 2021. Development of thick paste-like inks based on superconcentrated gelatin/alginate for 3D printing of scaffolds with shape fidelity and stability. Mater. Sci. Eng. C 122, 1–10. https://doi.org/10.1016/j.msec.2021.111866.

Datta, P., Barui, A., Wu, Y., Ozbolat, V., Moncal, K.K., Ozbolat, I.T., 2018. Essential steps in bioprinting: From pre- to post-bioprinting. Biotechnol. Adv. 36 (5), 1481–1504. https://doi.org/10.1016/j.biotechadv.2018.06.003.

Derakhshanfar, S., Mbeleck, R., Xu, K., Zhang, X., Zhong, W., Xing, M., 2018. 3D bioprinting for biomedical devices and tissue engineering: A review of recent trends and advances. Bioact. Mater. 3 (2), 144–156. https://doi.org/10.1016/j.bioactmat.2017.11.008.

Economidou, S.N., Lamprou, D.A., Douroumis, D., 2018. 3D printing applications for transdermal drug delivery. Int. J. Pharm. 544 (2), 415–424. https://doi.org/10.1016/j.ijpharm.2018.01.031.

Firth, J., Basit, A.W., Gaisford, S., 2018. The role of semi-solid extrusion printing in clinical practice. AAPS Adv. Pharm. Sci. Ser. 133–151. https://doi.org/10.1007/978-3-319-90755-0_7.

Freeman, F.E., Kelly, D.J., 2017. Tuning alginate bioink stiffness and composition for controlled growth factor delivery and to spatially direct MSC Fate within bioprinted tissues. Sci. Rep. 7, 1–12. https://doi.org/10.1038/s41598-017-17286-1.

Gao, T., Gillispie, G.J., Copus, J.S., Kumar, A., Rajan, P., Seol, Y., Atala, A., Yoo, J.J., Lee, S.J., 2019. Optmization of gelatin-alginate composite bioik printability using rheological parameters: a systematic approach. Biofabrication 10, 1–17. https://doi.org/10.1088/1758-5090/aacdc7.Optimization.

George, H.F., Qureshi, F., 2013. Newton's Law of Viscosity, Newtonian and Non-Newtonian Fluids. In: Wang, Q.J., Chung, Y.W. (Eds.), Encyclopedia of Tribology. Springer, Boston, MA, pp. 2416–2420. https://doi.org/10.1007/978-0-387-92897-5.

Gillispie, G., Prim, P., Copus, J., Fisher, J., Mikos, A.G., Yoo, J.J., Atala, A., Lee, S.J., 2020. Assessment Methodologies for Extrusion-Based Bioink Printability. Biofabrication 12, 1–28. https://doi.org/10.1088/1758-5090/ab6f0d.Assessment.

Godoi, F.C., Prakash, S., Bhandari, B.R., 2016. 3d Printing Technologies Applied for Food Design: Status and prospects. J. Food Eng. 179, 44–54. https://doi.org/10.1016/j.jfoodeng.2016.01.025.

Gopinathan, J., Noh, I., 2018. Recent trends in bioinks for 3D printing. Biomater. Res. 22, 1–15.

Gu, Z., Fu, J., Lin, H., He, Y., 2020. Development of 3D bioprinting: From printing methods to biomedical applications. Asian J. Pharm. Sci. 15 (5), 529–557. https://doi.org/10.1016/j.ajps.2019.11.003.

Habib, A., Sathish, V., Mallik, S., Khoda, B., 2018. 3D printability of alginate-carboxymethyl cellulose hydrogel. Materials (Basel). 11, 1–22. https://doi.org/10.3390/ma11030454.

Habib, M.A., Khoda, B., 2018. Development of clay based novel bio-ink for 3D bio-printing process. Proc. Manuf. 26, 846–856. https://doi.org/10.1016/j.promfg.2018.07.105.

He, Y., Yang, F., Zhao, H., Gao, Q., Xia, B., Fu, J., 2016. Research on the printability of hydrogels in 3D bioprinting. Sci. Rep. 6, 1–13. https://doi.org/10.1038/srep29977.

Jessop, Z.M., Al-Sabah, A., Gao, N., Kyle, S., Thomas, B., Badiei, N., Hawkins, K., Whitaker, I.S., 2019. Printability of pulp derived crystal, fibril and blend nanocellulose-alginate bioinks for extrusion 3D bioprinting. Biofabrication 11, 1–17. https://doi.org/10.1088/1758-5090/ab0631.

Jia, W., Gungor-Ozkerim, P.S., Zhang, Y.S., Yue, K., Zhu, K., Liu, W., Pi, Q., Byambaa, B., Dokmeci, M.R., Shin, S.R., Khademhosseini, A., 2016. Direct 3D bioprinting of perfusable vascular constructs using a blend bioink. Biomaterials 106, 58–68. https://doi.org/10.1016/j.biomaterials.2016.07.038.

Jiang, T., Munguia-Lopez, J.G., Flores-Torres, S., Kort-Mascort, J., Kinsella, J.M., 2019. Extrusion bioprinting of soft materials: An emerging technique for biological model fabrication. Appl. Phys. Rev. 6, 1–32. https://doi.org/10.1063/1.5059393.

Kang, K.H., Hockaday, L.A., Butcher, J.T., 2013. Quantitative optimization of solid freeform deposition of aqueous hydrogels. Biofabrication 5, 1–14. https://doi.org/10.1088/1758-5082/5/3/035001.

Kim, B.S., Kwon, Y.W., Kong, J.S., Park, G.T., Gao, G., Han, W., Kim, M.B., Lee, H., Kim, J.H., Cho, D.W., 2018. 3D cell printing of in vitro stabilized skin model and in vivo pre-vascularized skin patch using tissue-specific extracellular matrix bioink: A step towards advanced skin tissue engineering. Biomaterials 168, 38–53. https://doi.org/10.1016/j.biomaterials.2018.03.040.

Kim, M.H., Nam, S.Y., 2020. Assessment of coaxial printability for extrusion-based bioprinting of alginate-based tubular constructs. Bioprinting 20, 1–8. https://doi.org/10.1016/j.bprint.2020.e00092.

Kim, M.K., Jeong, W., Lee, S.M., Kim, J.B., Jin, S., Kang, H.-W., 2019. Decellularized extracellular matrix-based bio-ink with enhanced 3D printability and mecahnical properties. Biofabrication 2, 1–36.

Kirchmajer, D.M., Gorkin, R., Panhuis, I.H., M.,, 2015. An overview of the suitability of hydrogel-forming polymers for extrusion-based 3D-printing. J. Mater. Chem. B 3, 4105–4117. https://doi.org/10.1039/c5tb00393h.

Koch, F., Tröndle, K., Finkenzeller, G., Zengerle, R., Zimmermann, S., Koltay, P., 2020. Generic method of printing window adjustment for extrusion-based 3D-bioprinting to maintain high viability of mesenchymal stem cells in an alginate-gelatin hydrogel. Bioprinting 20, 1–9. https://doi.org/10.1016/j.bprint.2020.e00094.

Kotta, S., Nair, A., Alsabeelah, N., 2019. 3D Printing Technology in Drug Delivery: Recent Progress and Application. Curr. Pharm. Des. 24 (42), 5039–5048. https://doi.org/10.2174/1381612825666181206123828.

Kreller, T., Distler, T., Heid, S., Gerth, S., Detsch, R., Boccaccini, A.R., 2021. Physico-chemical modification of gelatine for the improvement of 3D printability of oxidized alginate-gelatine hydrogels towards cartilage tissue engineering. Mater. Des. 208, 1–13. https://doi.org/10.1016/j.matdes.2021.109877.

Lee, J., Unnithan, A.R., Park, C.H., Kim, C.S., 2019. In: Biomimetic Nanoengineered Materials for Advanced Drug Delivery. Elsevier, pp. 61–72. https://doi.org/10.1016/B978-0-12-814944-7.00005-9.

Lee, J.M., Sing, S.L., Zhou, M., Yeong, W.Y., 2018. 3D bioprinting processes: A perspective on classification and terminology. Int. J. Bioprinting 4, 1–10. https://doi.org/10.18063/IJB.v4i2.151.

Lee, S.C., Gillispie, G., Prim, P., Lee, S.J., 2020. Physical and Chemical Factors Influencing the Printability of Hydrogel-based Extrusion Bioinks. Chem. Rev. 120 (19), 10834–10886. https://doi.org/10.1021/acs.chemrev.0c00015.

Leucht, A., Volz, A.C., Rogal, J., Borchers, K., Kluger, P.J., 2020. Advanced gelatin-based vascularization bioinks for extrusion-based bioprinting of vascularized bone equivalents. Sci. Rep. 10, 1–15. https://doi.org/10.1038/s41598-020-62166-w.

Li, J., Wu, C., Chu, P.K., Gelinsky, M., 2020. 3D printing of hydrogels: Rational design strategies and emerging biomedical applications. Mater. Sci. Eng. R Reports 140, 1–76. https://doi.org/10.1016/j.mser.2020.100543.

Liu, W., Heinrich, M.A., Zhou, Y., Akpek, A., Hu, N., 2017. Extrusion Bioprinting of Shear-Thinning Gelatin Methacryloyl Bioinks. Physiol. Behav. 176, 139–148. https://doi.org/10.1002/adhm.201601451.Extrusion.

Liu, W., Zhong, Z., Hu, N., Zhou, Y., Maggio, L., Miri, A.K., Fragasso, A., Jin, X., Khademhosseini, A., Zhang, Y.S., Konkuk, T., 2019. Coaxial Extrusion Bioprinting of 3D Microfibrous Constructs with Cell-Favorable Gelatin Methacryloyl Microenvironments. Biofabrication 10, 1–18. https://doi.org/10.1088/1758-5090/aa9d44.Coaxial.

Magalhães, I.P., de Oliveira, P.M., Dernowsek, J., Casas, E.B.L., Casas, M.S.L., 2019. Investigation of the effect of nozzle design on rheological bioprinting properties using computational fluid dynamics. Rev. Mater. 24, 1–10. https://doi.org/10.1590/s1517-707620190003.0714.

Mohammed, A.A., Algahtani, M.S., Ahmad, M.Z., Ahmad, J., 2021. Optimization of semisolid extrusion (pressure-assisted microsyringe)-based 3D printing process for advanced drug delivery application. Ann. 3D Print Med. 2, 1–8. https://doi.org/10.1016/j.stlm.2021.100008.

Mouser, V.H.M., Melchels, F.P.W., Visser, J., Dhert, W.J.A., Gawlitta, D., Malda, J., 2016. Yield stress determines bioprintability of hydrogels based on gelatin-methacryloyl and gellan gum for cartilage bioprinting. Biofabrication 8, 1–13. https://doi.org/10.1088/1758-5090/8/3/035003.

Murphy, S.V., Atala, A., 2014. 3D bioprinting of tissues and organs. Nat. Biotechnol. 32 (8), 773–785. https://doi.org/10.1038/nbt.2958.

Naghieh, S., Chen, X., 2021. Printability – a Key Issue in Extrusion-based Bioprinting. J. Pharm. Anal. 11 (5), 564–579. https://doi.org/10.1016/j.jpha.2021.02.001.

Naghieh, S., Sarker, M.D., Sharma, N.K., Barhoumi, Z., Chen, X., 2019. Printability of 3D printed hydrogel scaffolds: Influence of hydrogel composition and printing parameters. Appl. Sci. 10, 1–18. https://doi.org/10.3390/app10010292.

Ngo, T.D., Kashani, A., Imbalzano, G., Nguyen, K.T.Q., Hui, D., 2018. Additive manufacturing (3D printing): A review of materials, methods, applications and challenges. Compos. Part B Eng. 143, 172–196. https://doi.org/10.1016/j.compositesb.2018.02.012.

O'Connell, C., Ren, J., Pope, L., Li, Y., Mohandas, A., Blanchard, R., Duchi, S., Onofrillo, C., 2017. In: Characterizing Bioinks for Extrusion Bioprinting: Printability and Rheology, 3D Bioprinting. Humana Press, pp. 111–251. https://doi.org/10.1016/c2014-0-02349-0.

Ouyang, L., Yao, R., Zhao, Y., Sun, W., 2016. Effect of bioink properties on printability and cell viability for 3D bioplotting of embryonic stem cells. Biofabrication 8, 1–12. https://doi.org/10.1088/1758-5090/8/3/035020.

Ozbolat, I.T., Peng, W., Ozbolat, V., 2016. Application areas of 3D bioprinting. Drug Discov. Today 21 (8), 1257–1271. https://doi.org/10.1016/j.drudis.2016.04.006.

Park, H.E., Gasek, N., Hwang, J., Weiss, D.J., Lee, P.C., 2020. Effect of temperature on gelation and cross-linking of gelatin methacryloyl for biomedical applications. Phys. Fluids 32, 1–12. https://doi.org/10.1063/1.5144896.

Park, J., Lee, S.J., Chung, S., Lee, J.H., Kim, W.D., Lee, J.Y., Park, S.A., 2017. Cell-laden 3D bioprinting hydrogel matrix depending on different compositions for soft tissue engineering: Characterization and evaluation. Mater. Sci. Eng. C 71, 678–684. https://doi.org/10.1016/j.msec.2016.10.069.

Pati, F., Jang, J., Lee, J.W., Cho, D.-W., 2015. In: Essentials of 3D Biofabrication and Translation. Elsevier, pp. 123–152. https://doi.org/10.1016/B978-0-12-800972-7.00007-4.

Paxton, N., Smolan, W., Bock, T., Melchels, F., Groll, J., Jungst, T., 2018. Porposal to Assess Printability of Bioinks for Extrusion-Based Bioprinting and Evaluation of Rheoogical Governing Bioprintability. Biofabrication 9, 1–33. https://doi.org/10.1088/1758-5090/aa8dd8.

Peng, W., Datta, P., Ayan, B., Ozbolat, V., Sosnoski, D., Ozbolat, I.T., 2017. 3D bioprinting for drug discovery and development in pharmaceutics. Acta Biomater. 57, 26–46. https://doi.org/10.1016/j.actbio.2017.05.025.

Pi, Q., Maharjan, S., Yan, X., Liu, X., Singh, B., van Genderen, A.M., Robledo-Padilla, F., Parra-Saldivar, R., Hu, N., Jia, W., Xu, C., Kang, J., Hassan, S., Cheng, H., Hou, X., Khademhosseini, A., Zhang, Y.S., 2018. Digitally Tunable Microfluidic Bioprinting of Multilayered Cannular Tissues. Adv. Mater. 30, 1–10. https://doi.org/10.1002/adma.201706913.

Prasad, L.K., Smyth, H., 2016. 3D Printing technologies for drug delivery: a review. Drug Dev. Ind. Pharm. 42 (7), 1019–1031. https://doi.org/10.3109/03639045.2015.1120743.

Ramesh, S., Harrysson, O.L.A., Rao, P.K., Tamayol, A., Cormier, D.R., Zhang, Y., Rivero, I.V., 2021. Extrusion bioprinting: Recent progress, challenges, and future opportunities. Bioprinting 21, 1–19. https://doi.org/10.1016/j.bprint.2020.e00116.

Ribeiro, A., Blokzijl, M.M., Levato, R., Visser, C.W., Castilho, M., Hennik, W.E., Vermonden, T., Malda, J., 2017. Assessment bioink shape fidelity to aid material development in 3D bioprinting. Biofabrication 10, 1–22. https://doi.org/10.1088/1758-5090/aa90e2.

Sarker, M., Chen, X.B., 2017. Modeling the Flow Behavior and Flow Rate of Medium Viscosity Alginate for Scaffold Fabrication With a Three-Dimensional Bioplotter. J. Manuf. Sci. Eng. 139, 1–32. https://doi.org/10.1115/1.4036226.

Schwab, A., Levato, R., D'Este, M., Piluso, S., Eglin, D., Malda, J., 2020. Printability and Shape Fidelity of Bioinks in 3D Bioprinting. Chem. Rev. 120 (19), 11028–11055. https://doi.org/10.1021/acs.chemrev.0c00084.

Seoane-Viaño, I., Januskaite, P., Alvarez-Lorenzo, C., Basit, A.W., Goyanes, A., 2021. Semi-solid extrusion 3D printing in drug delivery and biomedicine: Personalised solutions for healthcare challenges. J. Control. Release 332, 367–389. https://doi.org/10.1016/j.jconrel.2021.02.027.

Shahbazi, M., Jäger, H., 2021. Current Status in the Utilization of Biobased Polymers for 3D Printing Process: A Systematic Review of the Materials, Processes, and Challenges. ACS Appl. Bio Mater. 4 (1), 325–369. https://doi.org/10.1021/acsabm.0c01379.

Skardal, A., Devarasetty, M., Kang, H.W., Seol, Y.J., Forsythe, S.D., Bishop, C., Shupe, T., Soker, S., Atala, A., 2016. Bioprinting cellularized constructs using a tissue-specific hydrogel bioink. J. Vis. Exp. 1–8 https://doi.org/10.3791/53606.

Soltan, N., Ning, L., Mohabatpour, F., Papagerakis, P., Chen, X., 2019. Printability and Cell Viability in Bioprinting Alginate Dialdehyde-Gelatin Scaffolds. ACS Biomater. Sci. Eng. 5 (6), 2976–2987. https://doi.org/10.1021/acsbiomaterials.9b0016710.1021/acsbiomaterials.9b00167.s001.

Song, S.J., Choi, J., Park, Y.D., Lee, J.J., Hong, S.Y., Sun, K., 2010. A three-dimensional bioprinting system for use with a hydrogel-based biomaterial and printing parameter characterization. Artif. Organs 34, 1044–1048. https://doi.org/10.1111/j.1525-1594.2010.01143.x.

Suo, H., Zhang, J., Xu, M., Wang, L., 2021. Low-temperature 3D printing of collagen and chitosan composite for tissue engineering. Mater. Sci. Eng. C 123, 1–9. https://doi.org/10.1016/j.msec.2021.111963.

Therriault, D., White, S.R., Lewis, J.A., 2007. Rheological behavior of fugitive organic inks for direct-write assembly. Appl. Rheol. 17, 1–8. https://doi.org/10.1515/arh-2007-0001.

Theus, A.S., Ning, L., Hwang, B., Gil, C., Chen, S., Wombwell, A., Mehta, R., Serpooshan, V., 2020. Bioprintability: Physiomechanical and biological requirements of materials for 3d bioprinting processes. Polymers (Basel). 12, 1–19. https://doi.org/10.3390/polym12102262.

Townsend, J.M., Beck, E.C., Gehrke, S.H., Berkland, C.J., Detamore, M.S., 2019. Flow behavior prior to crosslinking: The need for precursor rheology for placement of hydrogels in medical applications and for 3D bioprinting. Prog. Polym. Sci. 91, 126–140. https://doi.org/10.1016/j.progpolymsci.2019.01.003.

Trenfield, S.J., Awad, A., Goyanes, A., Gaisford, S., Basit, A.W., 2018. 3D Printing Pharmaceuticals: Drug Development to Frontline Care. Trends Pharmacol. Sci. 39 (5), 440–451. https://doi.org/10.1016/j.tips.2018.02.006.

Unagolla, J.M., Jayasuriya, A.C., 2020. Hydrogel-based 3D bioprinting: A comprehensive review on cell-laden hydrogels, bioink formulations, and future perspectives. Appl. Mater. Today 18, 1–22. https://doi.org/10.1016/j.apmt.2019.100479.

Vithani, K., Goyanes, A., Jannin, V., Basit, A.W., Gaisford, S., Boyd, B.J., 2019. An Overview of 3D Printing Technologies for Soft Materials and Potential Opportunities for Lipid-based Drug Delivery Systems. Pharm. Res. 36, 1–50. https://doi.org/10.1007/s11095-018-2531-1.

Wang, L.L., Highley, C.B., Yeh, Y.-C., Galarraga, J.H., Uman, S., Burdick, J.A., 2018. 3D extrusion bioprinting of single- and double-network hydrogels containing dynamic covalent crosslinks. J. Biomed. Mater. Res. A 106, 1–21. https://doi.org/10.1002/jbm.a.36323.3D.

Wang, S., Lee, J.M., Yeong, W.Y., 2015. Smart hydrogels for 3D bioprinting. Int. J. Bioprinting 1, 3–14. https://doi.org/10.18063/IJB.2015.01.005.

Webb, B., Doyle, B.J., 2017. Parameter optimization for 3D bioprinting of hydrogels. Bioprinting 8, 8–12. https://doi.org/10.1016/j.bprint.2017.09.001.

Wu, D., Yu, Y., Tan, J., Huang, L., Luo, B., Lu, L., Zhou, C., 2018. 3D bioprinting of gellan gum and poly (ethylene glycol) diacrylate based hydrogels to produce human-scale constructs with high-fidelity. Mater. Des. 160, 486–495. https://doi.org/10.1016/j.matdes.2018.09.040.

You, F., Eames, B.F., Chen, X., 2017. Application of extrusion-based hydrogel bioprinting for cartilage tissue engineering. Int. J. Mol. Sci. 18, 8–14. https://doi.org/10.3390/ijms18071597.

Zhang, X., Liu, Y., Luo, C., Zhai, C., Li, Z., Zhang, Y.i., Yuan, T., Dong, S., Zhang, J., Fan, W., 2021. Crosslinker-free silk/decellularized extracellular matrix porous bioink for 3D bioprinting-based cartilage tissue engineering. Mater. Sci. Eng. C 118, 111388. https://doi.org/10.1016/j.msec.2020.111388.